On the topology design of a mechanical heterogeneous specimen using geometric and material nonlinearities

On the topology design of a mechanical heterogeneous specimen using geometric and material nonlinearities

M Gonçalves[1], A Andrade-Campos[1] and S Thuillier[2]

[1] Centre for Mechanical Technology and Automation (TEMA), Department of Mechanical Engineering, University of Aveiro, Portugal
[2] Univ. Bretagne Sud, UMR CNRS 6027, IRDL, F-56100, Lorient, France

E-mail: mafalda.goncalves@ua.pt, gilac@ua.pt, sandrine.thuillier@univ-ubs.fr

Abstract. Material characterization and the calibration of constitutive models play an important role in the majority of the forming processes nowadays. For an accurate virtualization of the processes, the material mechanical behavior needs to be known a priori. The classical characterization procedure involves carrying out several standard mechanical tests to identify the required information about the material. However, this procedure turns out to be expensive and time-consuming. Heterogeneous mechanical tests have been used to overcome this issue. By providing richer information with a reduced number of tests, their use can enhance the actual material characterization process. This work aims at making a significant contribution towards this goal by designing a heterogeneous mechanical test using topology optimization. A specimen topology is obtained with a heterogeneous displacement field by applying the theory of compliant mechanisms. Due to the large displacements considered, a geometrically nonlinear finite element analysis and a topology optimization procedure are proposed. Material nonlinearity is taken into account as well, to design solutions closer to reality. An optimal mechanical test with a highly heterogeneous strain field is obtained and evaluated, considering its diversity, using mechanism theory and a mechanical indicator.

1. Introduction

The virtualization of sheet metal forming processes is proceeding at an increasing pace. Material characterization and model calibration procedures play a key role in the accuracy of that process. A whole range of classical mechanical tests is usually carried out to identify the required parameters to characterize a specific material behavior. In order to avoid the costs and time associated with this procedure, heterogeneous mechanical tests have been used. Several authors have already addressed this topic by proposing nonstandard configurations for mechanical tests towards the improvement of the material characterization process. The design of a mechanical test based on the empirical knowledge of the authors was addressed in [1–3], for example. The strain field heterogeneity was used as a criterion to lead the design process using optimization methodologies [4–7]. A step further relies on evaluating the uncertainty of the identified parameters [8–10]. Adding the errors from full-field measurements techniques, the full measurement chain can be considered to evaluate the identification quality [11, 12].

Although several methodologies have already been proposed, to the best of the authors' knowledge, there is still a need for a systematic design methodology. An optimization approach

is required to achieve an optimal solution for the test design. Also, the obtained designs need to be independent on the initial guess of the design. Therefore, this work aims at filling this gap by proposing an nonlinear topology-based optimization methodology for designing specimen geometries with heterogeneous displacement and strain fields. The goal is to provide a relevant quantity and quality of information about the material behavior with a single test. The design methodology is based on a nonlinear topology optimization problem. Geometric and material nonlinearities are considered in order to account for the large displacements and the nonlinear material behavior. Several works have already addressed the nonlinear topology design of structures and compliant mechanisms. Topology optimization of structures with both geometric and material nonlinearities was addressed by Jung *et al.* [13]. Huang *et al.* [14] focused also on structural design under displacement loading. Capasso *et al.* [15] used nonlinear mechanics to analyze the stress-based topology optimization of compliant mechanisms. A similar work was proposed by Leon *et al.* [16], who also addressed the topology design of compliant mechanisms with material and geometric nonlinearities using stress constraints.

This work proposes a methodology to design specimen geometries with strain heterogeneities by coupling the design by topology optimization and an extended version of the theory of compliant mechanisms [17]. On this basis, non standard specimen designs can be obtained with highly heterogeneous displacement fields. Heterogeneity is introduced through the displacement field by applying two displacements in specific locations of the specimen. Therefore, several mechanical states can be induced depending on the applied displacements. A previous work already accounted for the large deformations that the specimen is submitted to [18]. In this work, material nonlinearity is introduced, being the nonlinear material behavior described by von Mises yield criterion and the Swift law. An optimal specimen geometry is obtained with a nonconventional geometry. Its performance in inducing a diversity of stress states is evaluated using a mechanical indicator.

2. Heterogeneous test design

Heterogeneous mechanical tests are a step ahead in material characterization due to the heterogeneous displacement and strain fields that are induced in them. These provide relevant information about the material behavior that is crucial for the calibration of the constitutive models. To induce such heterogeneity in a specimen is the goal of some of the test design methodologies that have been developed. In this work, it is proposed to introduce heterogeneity in the displacement field by coupling the design by topology optimization and an extended version of the compliant mechanisms. The former is used to obtain nonstandard specimen geometries, which on its own already can generate nonhomogeneous displacement fields. The latter is added to the approach to create more heterogeneity by applying displacements in specific locations of the specimen. Depending on the chosen locations, specific strain/stress states can be induced in the specimen and, consequently, lead to the enrichment of the strain field.

The design by topology optimization starts from a predefined design domain to find the optimal material distribution inside the boundaries of that domain. The starting point chosen in this work is represented in Figure 1. A schematic representation of the initial design domain is shown, which geometry is chosen in order not to restrict the material distribution update. A uniaxial tensile loading test is reproduced. Only one quarter of the design domain is represented. The load applied by the grips of the testing machine is represented by $\mathbf{F}_{\text{in}}$. The height of the design domain is more than twice than the height of the grips since it is assumed that this height is enough to provide the optimal solutions. Based on the theory of compliant mechanisms, two displacements are applied in specific locations of the specimen. Two locations, input and output, are chosen empirically by the authors. The first one corresponds to the displacement of the grips and the second is applied preferentially far from the specimen boundaries. It can be applied in different directions, being responsible for the way the specimen deforms.

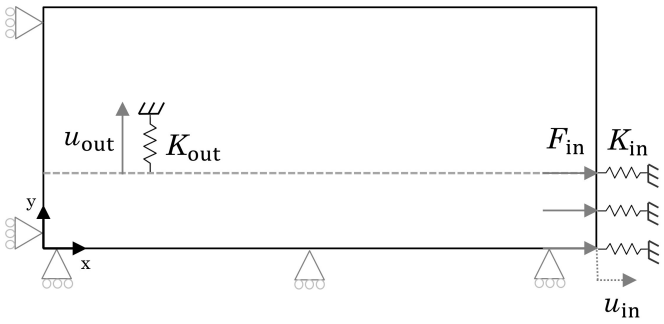

Figure 1: Schematic representation of the topology design domain subjected to a uniaxial tensile loading.

2.1. Problem formulation

The design optimization problem aims at finding the optimal material distribution for the specimen. The material layout, $\mathbf{X}$, is defined by the design variables, X_e, that represent the relative density of each element. These variables characterize the quantity of material in each element, taking the value 0 when the element is empty or the value 1 when the element is full. The density of each element is updated at each iteration of the optimization process until the optimum of the objective-function is found. In this work, it is proposed to maximize the ratio between the displacements in the output, u_{out}, and input, u_{in}, locations in order to enhance the heterogeneity of the displacement field of the specimen. Therefore, the optimization problem is defined as follows:

$$\begin{aligned} \underset{\mathbf{X}}{\text{maximize}} \quad & T(\mathbf{X}) = \frac{u_{\text{out}}(\mathbf{X})}{u_{\text{in}}(\mathbf{X})}, \\ \text{subject to} \quad & \mathbf{R} = \mathbf{0}, \\ & \frac{\sum_{e=1}^{M} X_e V_e}{\sum_{e=1}^{M} V_e} - V^* \leq 0, \\ & 0 \leq \rho_{\min} \leq X_e \leq 1, \ e = 1, 2, .., M. \end{aligned} \tag{1}$$

where M is the number of elements and V_e the volume fraction of each one. V^* corresponds to the volume fraction required for the final specimen design. $\rho_{\min}$ represents a minimum value for the element density to avoid numerical issues. A nonlinear finite element analysis is proposed for the design procedure. When the equilibrium is achieved, the balance between the external and internal loads of the specimen, $\mathbf{R} = 0$, is required to be zero.

2.2. Nonlinear Finite Element Analysis

To reproduce accurately the specimen behavior when submitted to a tensile loading test, it is proposed to carry out a nonlinear finite element analysis. Both material and geometric nonlinearities are considered and the latter aims at accounting for the large displacements that the specimen is submitted to. For that purpose, the Green-Lagrange strain tensor is used, being composed of linear and nonlinear parts that can be represented as follows:

$$\mathbf{E} = \mathbf{E}_{\text{L}} + \mathbf{E}_{\text{N}} \ = \ \mathbf{B}_{\text{L}}\mathbf{U} + \mathbf{B}_{\text{N}}\mathbf{U}, \tag{2}$$

where $\mathbf{B}_{\text{L}}$ and $\mathbf{B}_{\text{N}}$ correspond to the linear and nonlinear transformation matrices between nodal displacements, $\mathbf{U}$, and element strains, $\mathbf{E}$, respectively. Along with the strain measure, the sec-

ond Piola-Kirchoff stress tensor, $\mathbf{S}$, is also employed in the system analysis.

The equilibrium of the system is one of the constraints of the optimization procedure and can be defined as

$$\mathbf{R} = \int \mathbf{B}^{\mathrm{T}}\mathbf{S}\, dV - \mathbf{F}_{\mathrm{ext}} = \mathbf{F}_{\mathrm{int}} - \mathbf{F}_{\mathrm{ext}}, \tag{3}$$

where $\mathbf{B}$ is composed of both the linear and nonlinear matrices, $\mathbf{B}_{\mathrm{L}}$ and $\mathbf{B}_{\mathrm{N}}$, respectively. An incremental-iterative approach is used to solve the nonlinear finite element analysis. The external load is applied in increments $\Delta\mathbf{F}_{\mathrm{ext}}$ during which the displacements $\Delta\mathbf{U}$ are found iteratively to achieve the equilibrium for the current configuration. At each load increment, the equilibrium is achieved when the residual $\mathbf{R}$ is equal to zero. Its computation considers the current state of the topology, being $\mathbf{F}_{\mathrm{int}}$ the internal load of the system considering its history and $\mathbf{F}_{\mathrm{ext}}$ the load that has already been applied. The iterative procedure is solved using the Newton-Raphson algorithm and requires the determination of the tangent stiffness matrix defined as

$$\mathbf{K}_{\mathrm{T}} = -\frac{\partial \mathbf{R}}{\partial \mathbf{U}}, \tag{4}$$

that can be written as follows

$$\begin{aligned} \mathbf{K}_{\mathrm{T}} &= \mathbf{K}_{\mathrm{L}} + \mathbf{K}_{\mathrm{N}} + \mathbf{K}_{\mathrm{S}} \\ &= \int \mathbf{B}_{\mathrm{L}}^{\mathrm{T}}\mathbf{D}_{\mathrm{ep}}\mathbf{B}_{\mathrm{L}}dV + \int \mathbf{B}_{\mathrm{L}}^{\mathrm{T}}\mathbf{D}_{\mathrm{ep}}\mathbf{B}_{\mathrm{N}}dV + \int \mathbf{B}_{\mathrm{N}}^{\mathrm{T}}\mathbf{D}\mathbf{B}_{\mathrm{L}}dV + \int \mathbf{B}_{\mathrm{N}}^{\mathrm{T}}\mathbf{D}_{\mathrm{ep}}\mathbf{B}_{\mathrm{N}}dV + \int \mathbf{G}^{\mathrm{T}}\mathbf{M}\mathbf{G}dV. \end{aligned} \tag{5}$$

The first two terms, $\mathbf{K}_{\mathrm{L}}$ and $\mathbf{K}_{\mathrm{N}}$, are the stiffness matrices due to the small and large displacements, respectively. The latter term, $\mathbf{K}_{\mathrm{S}}$, is related to the initial stress state, in which $\mathbf{M}$ is composed of elements of the stress tensor $\mathbf{S}$ and $\mathbf{G}$ stands for a derivative matrix of shape functions with respect to coordinates. The consistent tangent matrix, represented as $\mathbf{D}_{\mathrm{ep}}$, improves the overall convergence of the equilibrium equations when the Newton-Raphson method is used for the latter [19]. It is computed during the material behavior analysis that will be described in the following section, considering plane stress conditions.

2.3. Material behavior

The elastoplastic material behavior is taken into account in this work. Both the elastic and the plastic behaviors are considered isotropic, being the former described by Hooke's law. The yield function can be represented as follows:

$$f(\boldsymbol{\sigma}, \bar{\varepsilon}^{\mathrm{p}}) = \sigma_{\mathrm{vm}}(\boldsymbol{\sigma}) - \sigma_y(\bar{\varepsilon}^{\mathrm{p}}) \tag{6}$$

where $\sigma_{\mathrm{vm}}(\boldsymbol{\sigma})$ stands for the von Mises equivalent stress defined based on the stress tensor $\boldsymbol{\sigma}$. The yield stress, represented as σ_y, is defined by the equivalent plastic strain, $\bar{\varepsilon}^{\mathrm{p}}$. Thus, the isotropic hardening behavior of the material is characterized by the Swift Law, which can be computed as

$$\sigma_y(\bar{\varepsilon}^{\mathrm{p}}) = K(\varepsilon_0 + \bar{\varepsilon}^{\mathrm{p}})^n \tag{7}$$

where K, ε_0 and n are the constitutive model parameters. The yield surface is described by the von Mises yield criterion [20] considering plane stress conditions as

$$\sigma_{\mathrm{vm}}(\boldsymbol{\sigma}) = \sqrt{\sigma_{xx}^2 + \sigma_{yy}^2 - \sigma_{xx}\sigma_{yy} + 3\tau_{xy}^2} \tag{8}$$

where σ_{xx}, σ_{yy} and τ_{xy} correspond to the components from Cauchy stress tensor $\boldsymbol{\sigma}$.

In the finite element analysis, the second Piola-Kirchhoff stress tensor, $\mathbf{S}$, is used (work-conjugate to the Green's strain tensor) in contrast to the Cauchy stresses, $\boldsymbol{\sigma}$, that are applied in the analysis of the material behavior. While the first one is related to the original configuration, the latter relates to the current configuration [19]. Therefore, it is needed to establish a relationship between them that is given by

$$\mathbf{S} = J\mathbf{F}^{-1}\boldsymbol{\sigma}\mathbf{F}^{-\mathrm{T}}, \tag{9}$$

where $\mathbf{F}$ is the deformation gradient between the original and the new configurations and J its determinant.

2.4. Sensitivity analysis

The objective-function of the topology optimization problem evaluates the ratio between the displacements in the output and input locations. Therefore, the sensitivity of the objective-function can be defined as

$$\frac{dT}{d\mathbf{X}} = \frac{\frac{du_{\mathrm{out}}}{d\mathbf{X}}u_{\mathrm{in}} - \frac{du_{\mathrm{in}}}{d\mathbf{X}}u_{\mathrm{out}}}{u_{\mathrm{in}}^2}, \tag{10}$$

where the derivative of the output and input displacements can be derived using the adjoint variable method in the following manner,

$$u_{\mathrm{in}} = \mathbf{L}_{\mathrm{in}}^{\mathrm{T}}\mathbf{U} + \boldsymbol{\gamma}^{\mathrm{T}}\mathbf{R}, \tag{11}$$

$$u_{\mathrm{out}} = \mathbf{L}_{\mathrm{out}}^{\mathrm{T}}\mathbf{U} + \boldsymbol{\lambda}^{\mathrm{T}}\mathbf{R}, \tag{12}$$

where $\mathbf{L}_{\mathrm{in}}$ and $\mathbf{L}_{\mathrm{out}}$ stand for two vectors with the value of one at the input and output locations and zeros in the remaining ones, respectively. Assuming that the equilibrium has been found, the terms $\boldsymbol{\gamma}^{\mathrm{T}}\mathbf{R}$ and $\boldsymbol{\lambda}^{\mathrm{T}}\mathbf{R}$ are equal to zero and, therefore can be added to the displacements. The derivative of the input and output displacements can be written as

$$\frac{\partial u_{\mathrm{in}}}{\partial X_e} = -p\left[(1-X_e)\,\rho_{\mathrm{min}}^{p-1} + X_e\right]\boldsymbol{\gamma}_e^{\mathrm{T}}\mathbf{F}_{\mathrm{int}}^e, \tag{13}$$

and

$$\frac{\partial u_{\mathrm{out}}}{\partial X_e} = -p\left[(1-X_e)\,\rho_{\mathrm{min}}^{p-1} + X_e\right]\boldsymbol{\lambda}_e^{\mathrm{T}}\mathbf{F}_{\mathrm{int}}^e, \tag{14}$$

respectively. The adjoint vectors $\boldsymbol{\lambda}$ and $\boldsymbol{\gamma}$ can be easily obtained as the solutions to the linear adjoint equations $\mathbf{K}_{\mathrm{T}}\boldsymbol{\lambda} = \mathbf{L}_{\mathrm{out}}$ and $\mathbf{K}_{\mathrm{T}}\boldsymbol{\gamma} = \mathbf{L}_{\mathrm{in}}$. The tangent stiffness matrix has already been found during the equilibrium equations. The material properties are determined using the Solid Isotropic Material with Penalization (SIMP) method [21], in which the element densities are penalized using a penalization factor, p. The adopted methodology [22] establishes a non-homogenized combination of solid and void in intermediate elements, being required a linear interpolation between the two phases, solid and void.

2.5. Solution evaluation

From the design optimization procedure, an optimal specimen geometry is obtained. Based on the stress/strain fields that are induced after a uniaxial tensile loading test, the specimen is evaluated using a mechanical indicator [7]. It analyzes the performance of the specimen in inducing a high diversity of stress states and can be computed as

$$id = \prod_{s=1}^{3}\left[\frac{3}{\sum_{e=1}^{n}X_e}\sum_{e=1}^{n}\left({}^{s}\delta_e\ Z_e\ X_e\right)\right]. \tag{15}$$

Solutions with stress concentrations or unstressed material are penalized based on the von Mises stress using the parameter Z_e. The index s indicates the stress state (tension, compression, and shear) that the element e is subjected to. According to the principal strains relationships, the operator ${}^s\delta_e$ assumes the value of one or zero if the element is in the stress state s or not, respectively. Based on a generalization of the smooth Heaviside function, the parameter ${}^s\delta_e$ can defined as

$$ {}^s\delta_e = \begin{cases} \frac{1}{2}\Big(1-\tanh\big(\beta\left(\varepsilon_e^1+0.75\varepsilon_e^2\right)\big)\Big), & s=1 \\ \frac{1}{4}\Big(1+\tanh\big(\beta\left(\varepsilon_e^1+0.75\varepsilon_e^2\right)\big)\Big)\Big(1-\tanh\big(\beta\left(\varepsilon_e^1+1.5\varepsilon_e^2\right)\big)\Big), & s=2\,. \\ \frac{1}{2}\Big(1+\tanh\big(\beta\left(\varepsilon_e^1+1.5\varepsilon_e^2\right)\big)\Big), & s=3 \end{cases} \tag{16} $$

where the parameter β controls the "agressiveness" of the Heaviside function. ε^1 and ε^2 stand for the major and minor principal strains, respectively. The ideal solution would present the same amount of material in the three stress states (tension, compression, and shear) without stress concentrations or unstressed material.

3. Implementation

The design procedure is based on a nonlinear topology-based optimization methodology from which an optimal specimen is obtained. Figure 2 represents the structure of the developed methodology.

At the beginning of the design optimization, the design domain is established along with the volume fraction and the filtering parameters [22]. The material distribution that is being evaluated is submitted to a nonlinear finite element analysis, from which the displacements and internal forces are obtained. The sensitivity analysis is performed as well as the objective-function computation. A filtering technique is applied to the sensitivities and the design variables are updated by the Method of Moving Asymptotes (MMA) [23]. A new iteration starts with the updated topology in case the convergence criterion is not reached. Otherwise, an optimal solution is obtained. At the end of this process, the solution is submitted to a performance evaluation using the mechanical indicator.

A nonlinear finite element analysis is proposed to account for the nonlinear behavior of the specimen. Since material and geometric nonlinearities are considered, an incremental analysis is proposed to evaluate the structure behavior as the load level evolves. The equilibrium $\mathbf{R}=\mathbf{0}$ is found, at each increment, iteratively using the Newton-Raphson method [19]. The tangent stiffness matrix describes the structure current configuration, being updated at each iteration. The equilibrium at each load increment is achieved when a balance between the external and internal loads is obtained. For determining the last ones, the computation of the stresses is required. The elastoplastic behavior of the material makes it necessary to use an yield criterion to predict when yielding occurs and, consequently, to compute correctly the stresses. If the stresses are computed by an elastic relationship and they are found to lie within the yield surface, the material is found to remain elastic. Otherwise, these are already in the plastic regime, being no longer determined by a linear assumption. The Backward-Euler return method [19] needs to be applied to determine the plastic strain increment and, consequently, the updated stresses and the consistent tangent matrix.

4. Results

The developed methodology is applied to the design of an optimal heterogeneous mechanical test. From the initial design domain, represented in Figure 1, three specimen geometries are obtained considering material and geometric nonlinearities. These solutions are shown in Figure 3. A

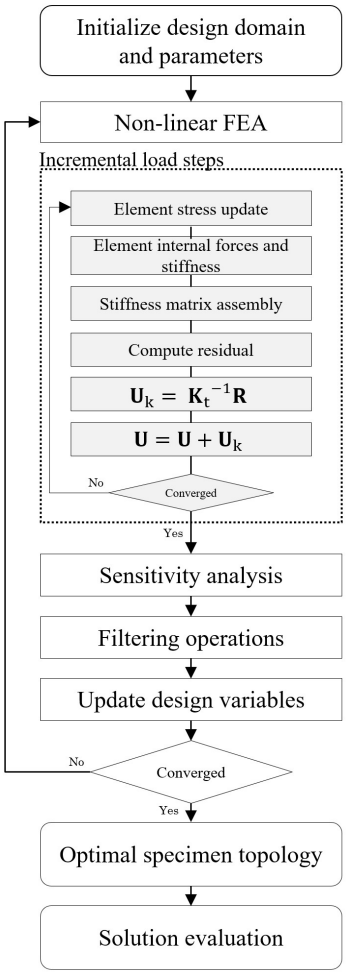

Figure 2: Flow diagram of the nonlinear topology optimization methodology.

volume fraction of 35% of the total initial volume is required for the specimen designs. The location of the output displacement is chosen to be established in the left symmetry boundary of the specimen and it is represented by the red arrow. A mesh of 50×50 elements is used. These parameters are the ones that led to the best results [24]. The elastic material properties are represented in Table 1 as well as the constitutive model parameters related to the Swift Law.

Table 1: Elastic properties and constitutive model parameters for Swift's isotropic hardening law of DP600 [25].

	Elastic		Swift		
	E [GPa]	ν	K [MPa]	ε_0	n
DP600	210	0.3	979.46	0.00535	0.194

Three different assumptions have led to the topologies presented in Figures 3(a), (b) and (c), that are entitled as solutions A, B and C, respectively. The first one considered the material behavior linear elastic. With the same material behavior, solution B was obtained assuming

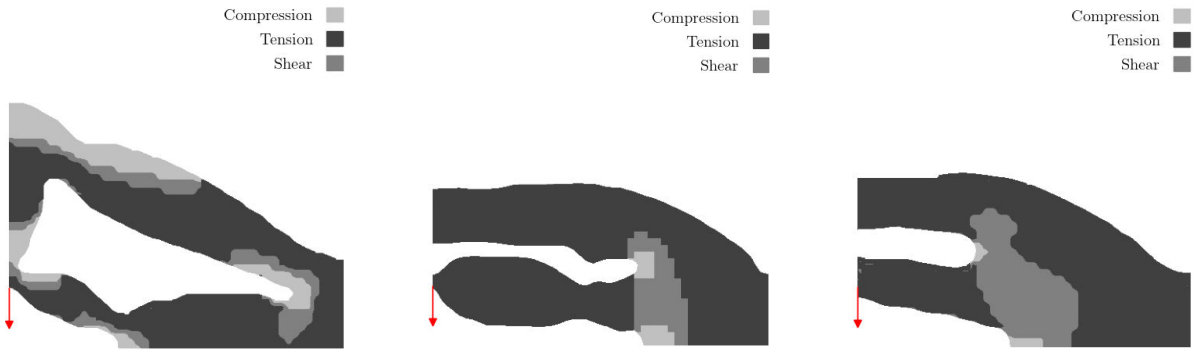

(a) Solution A (b) Solution B (c) Solution C

Figure 3: Obtained specimen designs with a topology-based optimization methodology considering: (a) a linear material and geometric behavior, (b) geometric nonlinearities with a linear elastic material and (c) geometric and material nonlinearities. The stress states induced in the specimen are represented.

geometric nonlinearities in order to account for the large displacements that the specimen is submitted to. Material and geometric nonlinearities were considered to obtain the last topology. The elastoplastic material behavior influences the design optimization process and, consequently, the obtained specimen designs.

Regarding the obtained specimen geometries, although the material is similarly placed in the locations where the displacements and loads are being applied, the overall material distribution is rather different. Their performance in inducing a high diversity of stress states is evaluated using the performance indicator. For the solutions A, B and C, the values of the performance indicator are 0.0359, 0.0190 and 0.0215, respectively, being the solution A the one with the highest heterogeneity of stress states. However, this scalar indicator does not take into consideration the equivalent plastic strain through the specimen or the duration of the test, since an early rupture of the specimen limits the quantity and quality of the information that can be extracted from the specimen. Therefore, a Finite Element Analysis (FEA) was conducted in ABAQUS/Standard using a forming limit diagram to predict the moment which the specimen rupture occurs. In Figure 4, the obtained results are represented. The ratio of the major and minor principal strains ($\varepsilon^1/\varepsilon^2$), the equivalent plastic strain ($\bar{\varepsilon}^{\mathrm{p}}$) and the von Mises stress (σ_{VM}) are depicted for each solution at the moment just before rupture.

Concerning the ratio between the major and minor principal strains, it can be noticed that due to the applied tensile load, most of the specimen is subjected to tension. However, a significant area of the specimens under other mechanical states, such as compression and shear (the mechanical states considered in this work) can be observed, particularly, in solution C. This validates the purpose of this methodology that aims at creating heterogeneity of mechanical states. The equivalent plastic strain is represented along the specimen at the moment just before rupture. In solution A, the rupture occurs too early in the testing procedure due to its complex geometry. Therefore, plastic strains only exists in small areas of the specimen. A similar issue arises in solution B. The solution C consists in the specimen geometry with the largest area in the plastic regime. Regarding the von Mises stress, the maximum values of each solution are similar, being around 700 MPa. Solution A, due to its early rupture in specific locations of the geometry, presents the maximum value in those locations, being most of the specimen area under low values of the von Mises stress. In contrast, the specimen C presents higher values of the von Mises stress over its surface, leading to a higher duration of the test and, consequently, providing more information about the material behavior.

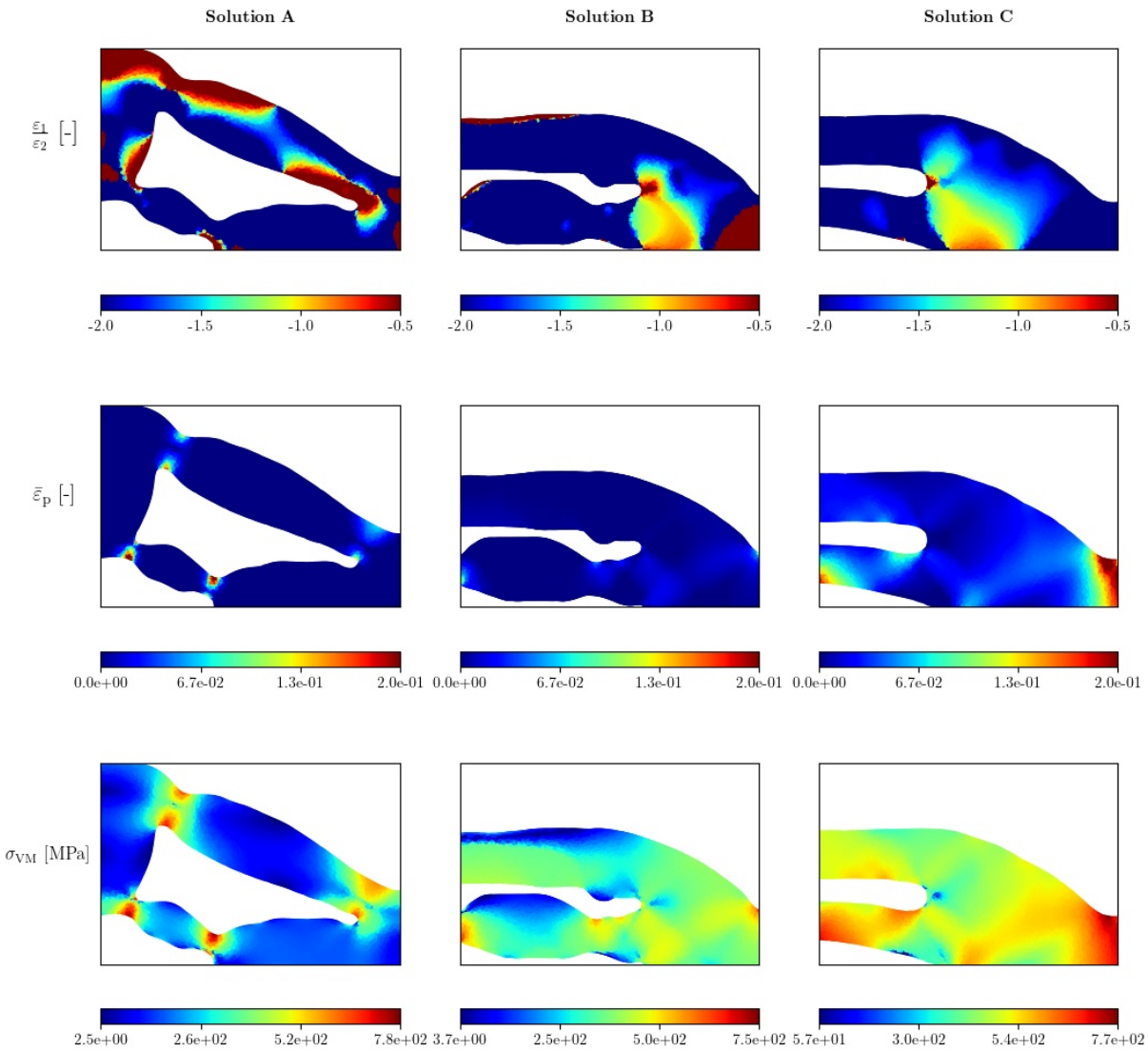

Figure 4: Obtained results from FEA: the ratio between major and minor principal strains ($\varepsilon^1/\varepsilon^2$), the equivalent plastic strain ($\bar{\varepsilon}^p$) and the von Mises stress (σ_{VM}) for each solution (A, B and C).

Based on these results, it is possible to conclude that the solution C, obtained with the methodology proposed in this work, consists in the specimen design that better suits for the improvement of the material characterization process. Therefore, this methodology should be used in order to obtain specimen geometries that take into account the real nonlinear material and geometric behavior.

5. Conclusions

In this work, a nonlinear topology-based methodology is proposed for the design of a heterogeneous mechanical test. Geometric and material nonlinearities are considered for the design of test in order to lead to more realistic results. Large deformations are taken into account in the finite element analysis as well as the elastoplastic material behavior, characterized by the von Mises yield criterion and the Swift law. An optimal specimen geometry is obtained.

The influence of the material and geometric nonlinearities in the test design is analyzed by comparing to other solutions. Several differences were noticed between the topologies related to the material layout and, consequently, to their performance. Solution C, the one obtained assuming a nonlinear material and geometric behavior, presented the largest area in the plastic regime and the more interesting von Mises stress distribution. The obtained specimen design has the potential to provide a higher quality and quantity of information about the material behavior, being the proposed methodology of major relevance for an accurate test design.

Acknowledgments

This project has received funding from the Research Fund for Coal and Steel under grant agreement No 888153. The authors also gratefully acknowledge the financial support of the Portuguese Foundation for Science and Technology (FCT) under the projects CENTRO-01-0145-FEDER-029713, POCI-01-0145-FEDER-031243 and POCI-01-0145-FEDER-030592 by UE/FEDER through the programs CENTRO 2020 and COMPETE 2020, and UIDB/00481/2020 and UIDP/00481/2020-FCT under CENTRO-01-0145-FEDER-022083. M. Gonçalves is grateful to the FCT for the Ph.D. grant Ref. UI/BD/151257/2021.

References

[1] Haddadi H and Belhabib S 2012 *Int. J. Mech. Sci.* **62** 47–56
[2] Belhabib S, Haddadi H, Gaspérini M and Vacher P 2008 *Int. J. Mech. Sci.* **50** 14–21
[3] Pottier T, Vacher P, Toussaint F, Louche H and Coudert T 2012 *Exp. Mech.* **52** 951–963
[4] Souto N, Andrade-Campos A and Thuillier S 2016 *Int. J. Mech. Sci.* **107** 264–276
[5] Andrade-Campos A, Aquino J, Martins J M and Coelho B 2019 *Metals* **9**
[6] Aquino J, Andrade-Campos A, Martins J M and Thuillier S 2019 *Strain* **55** 1–18
[7] Barroqueiro B, Andrade-Campos A, Dias-de Oliveira J and Valente R A 2020 *Int. J. Mech. Sci.* **181** 105764
[8] Pierron F, Vert G, Burguete R, Avril S, Rotinat R and Wisnom M R 2007 *Strain* **43** 250–259
[9] Bertin M B, Hild F and Roux S 2016 *Strain* **52** 307–323
[10] Chamoin L, Jailin C, Diaz M and Quesada L 2020 *Int. J. Solids Struct.* **193-194** 270–286
[11] Rossi M, Badaloni M, Lava P, Debruyne D and Pierron F 2016 *AIP Conf. Proc.* vol 1769
[12] Wang P, Pierron F, Rossi M, Lava P and Thomsen O T 2016 *Strain* **52** 59–79
[13] Jung D and Gea H C 2004 *Finite Elem. Anal. Des.* **40** 1417–1427
[14] Huang X and Xie Y M 2008 *Eng. Struct.* **30** 2057–2068
[15] Capasso G, Morlier J, Charlotte M and Coniglio S 2020 *Mech. Ind.* **21**
[16] De Leon D M, Gonçalves J F and de Souza C E 2020 *Struct. Multidiscip. Optim.* **62**
[17] Zhu B, Zhang X, Zhang H, Liang J, Zang H, Li H and Wang R 2020 *Mech. Mach. Theory* **143** 103622
[18] Gonçalves M, Andrade-Campos A and Thuillier S 2022 *Proceedings of the 25th ESAFORM conference*
[19] Crisfield M A 1991 *Non-Linear Finite Element Analysis of Solids and Structures, Essentials* (Wiley)
[20] Mises R v 1913 *Nachr. Ges. Wiss. Göttingen, Math.-Phys. Kl.* **1913** 582–592
[21] Rozvany G, Zhou M and Birker T 1992 *Struct. Multidiscip. Optim.* **4** 250–252
[22] Fu Y F, Rolfe B, Chiu L N N, Wang Y, Huang X and Ghabraie K 2020 *Adv. Eng. Softw.* **150** 102921
[23] Svanberg K 2009 *Encyclopedia of Optimization* ed Floudas C A and Pardalos P M (Boston, Massachusetts: Springer) pp 3832–3834
[24] Gonçalves M, Andrade-Campos A and Dias-de Oliveira J A 2021 *XVI International Conference on Computational Plasticity. Fundamentals and Applications* (Barcelona, Spain)
[25] Ozturk F, Toros S and Kilic S 2014 *Procedia Manuf.* **81** 760–765